

Electroactive hydrodynamic weirs for microparticle manipulation and patterning

Brian M. Taff,^{1,2} Salil P. Desai,¹ and Joel Voldman^{1,a)}

¹Department of Electrical Engineering and Computer Science, Massachusetts Institute of Technology, Cambridge, Massachusetts 02139, USA

²Department of Systems Biology, Harvard Medical School, Boston, Massachusetts 02115, USA

(Received 26 December 2008; accepted 27 January 2009; published online 24 February 2009)

We present a platform for parallelized manipulations of individual polarizable micron-scale particles (i.e., microparticles) that combines negative dielectrophoretic forcing with the passive capture of hydrodynamic weir-based trapping. Our work enables manipulations using ejection- and/or exclusion-based methods. In ejection operations, we unload targeted weirs by displacing microparticles from their capture faces via electrode activation. In exclusion-based operations, we prevent weir loading by activating selected on-chip electrodes before introducing microparticles into the system. Our work describes the device's passive loading dynamics and demonstrates enhanced functionalities by forming a variety of particle patterns. © 2009 American Institute of Physics. [DOI: 10.1063/1.3085955]

A number of techniques enable the placement and organization of micron-scale particles on a common substrate.¹⁻³ Dielectrophoresis (DEP) is one prevalent strategy for exerting forces in such contexts.^{4,5} DEP forces arise from localized nonuniform electric fields typically produced by applying voltages across collections of on-chip electrodes. These nonuniform fields induce dipoles and higher-order moments in polarizable particles positioned within such environments.⁶ The fields, in turn, exert forces on these moments to attract positive-DEP (*p*-DEP) or repel negative-DEP (*n*-DEP) particles toward or away from electric-field maxima. With this flexibility, one can engineer DEP-based platforms for a variety of particle sorting⁷ and patterning⁸ needs.

In recent years, researchers have developed a set of orthogonal but complementary weir-based methods for handling microparticles in fluidic microsystems.^{9,10} These approaches sequester individual particles to designated on-chip locations using mechanical barriers (or traps). After single particles load into individual traps, their presence alters the local hydrodynamic flow profiles such that subsequent impinging particles progress around loaded weirs, enabling the capture and retention of a single particle in each trap.

DEP and weir-based particle manipulation strategies provide unique sets of capabilities that to date, have not been combined. Most DEP-based efforts for organizing arrays of microparticles incorporate *p*-DEP strategies,^{11,12} which can be designed simply by placing electrodes at locations where on-chip capture is needed. Unfortunately, this approach requires low-conductivity buffers that can limit the assays performed in such systems. Though *n*-DEP functions in higher-conductivity buffers, developing manipulation platforms that use *n*-DEP is often challenging since *n*-DEP optimally repels particles. Furthermore, operation in high-conductivity solutions requires larger operating currents which limit scalability. Weir-based designs alternatively offer single-particle capture without imposing restrictions regarding buffer composition or a need for on-chip electrodes. Unfortunately,

without on-chip activation, the inherent static nature of such topologies renders them incapable of manipulating particles during or after loading.

Here we present a device architecture that combines the control enabled by *n*-DEP-based sorting with the effective single-particle capture offered by weirs (Fig. 1). In this system, we decouple capture and sorting by assigning each to an independent physical domain. We manage particle capture and retention using weirs and we achieve single-particle sorting via *n*-DEP forcing. This design partitioning enables manipulations in buffer solutions with a wide range of electrical properties. This approach furthermore reduces the current necessary for device operation compared to what would be needed for scaling prior *n*-DEP-based particle manipulation efforts; instead of turning all electrodes on at once to ensure particle capture and retention, we only activate electric fields in targeted locations to sort from designated subsets of traps.

Our active designs modulate array site loading and/or particle retention by using *n*-DEP forces to push particles away from selected weir capture crevices. With such forcing, passing fluid flow can sweep repelled particles out of the

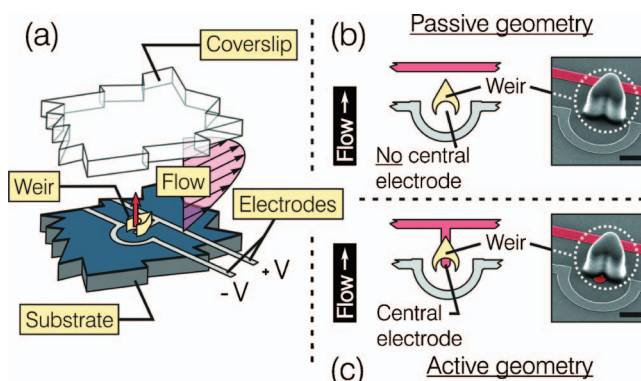


FIG. 1. (Color) (a) Depiction of the electroactive weirs, showing the electrodes used to exert *n*-DEP forces. [(b) and (c)] Schematic and pseudocolored SEM images of passive and active designs where the respective absence or presence of a central electrode regulates the ability to repel particles from weir capture crevices. (Scale bars=20 μm ; weirs formed using photopatterned silicone).

^{a)}Electronic mail: voldman@mit.edu.

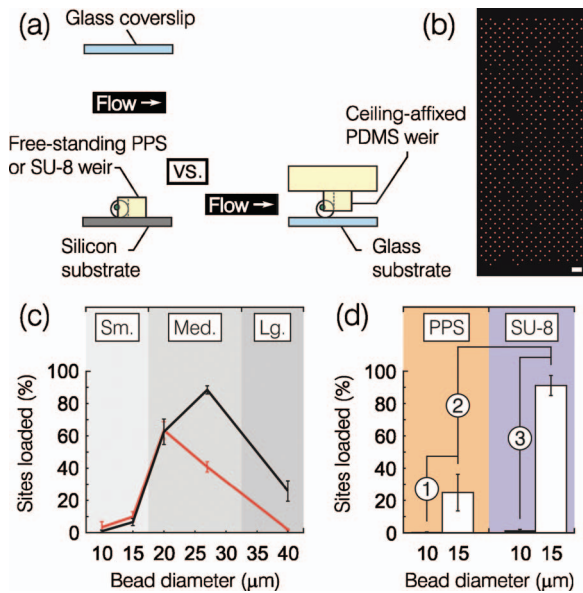


FIG. 2. (Color) (a) Side-view schematic comparing our large-gap weirs (left) with prior small-gap weirs (right). (b) Image of 27 μm diameter fluorescent beads loaded into an array of large-gap PPS weirs (scale bar = 180 μm). (c) Percentages of PPS weir sites loaded as a function of bead size at low (50 $\mu\text{l}/\text{min}$, black curve) and high (125 $\mu\text{l}/\text{min}$, red curve) flow rates (device flow chambers: 4 mm wide and ~ 250 μm high; results are averaged over three to four runs; error bars = ± 1 σ ; weir heights = 20 μm). (d) Comparisons of loading across two material systems and two bead diameters showing that large beads trap better in both device types (1 and 3) but that SU-8 weirs offer statistically significant enhancements in loading (2) for this examined particle size range.

device. Contrasting prior weir-based designs that incorporate ceiling-mounted polydimethylsiloxane weirs^{9,10} and narrow fluid gaps to generate stable single-particle traps, we have developed an alternative strategy where we fabricate weirs as substrate-affixed geometries formed in either photoresist (SU-8 2015, MicroChem Corp., Newton, MA) or a photopatternable silicone (PPS) (Ref. 13) [Fig. 2(a), supplemental Fig. 1 (Ref. 14)]. Our strategy creates large gaps between the tops of each weir and the channel ceiling providing room for particles to eject vertically out of the weirs when sorting. By creating weirs using photopatterning instead of the bulk molding processes implemented in prior efforts, we can readily align our weirs to prepatterned wafer substrates. We thus fabricate our devices on silicon and position individual weirs over a series of electrodes that provide the n -DEP forcing required for active sorting. The designs include a central electrode located beneath each capture crevice and a surrounding semicircular electrode driven with opposing polarity [Fig. 1(c)]. Such designs focus field flux through a narrow region within the capture crevice enabling electrical control over loading and/or retention responses.

While the loading mechanics of narrow-gap designs have been shown,^{9,10} the capture performance of large-gap weirs has not been reported. We ran a series of loading assays using devices incorporating arrays of over 600 passive weir geometries (lacking site unloading electrodes) and found that we could readily trap large numbers of individual polystyrene beads [Fig. 2(b), supplemental Fig. 2 (Ref. 14)]. Interestingly, we discovered through repeated assays run at varying flow rates, that our large-gap PPS-based weirs displayed size-selective loading responses where beads with diameters in the 20–30 μm range offered enhanced

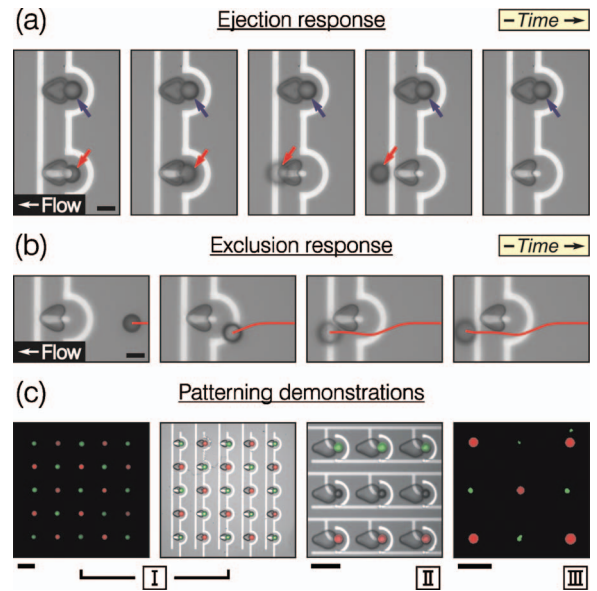


FIG. 3. (Color) Time-sequence images of particle ejection (a) and particle exclusion (b) from PPS electroactive weirs. For particle ejection, we show the site-specific repulsion of a captured particle from an active site (red arrow) and neighboring retention at a passive site (blue arrow). For particle exclusion, we activate electrodes (on state) prior to introducing particles, preventing site loading altogether. (Scale bars = 30 μm ; buffer = DI:PBS mixture at $\sigma = 0.5$ S/ma; $V = 2$ V_{pp} at 500 KHz.) (c) Images using electroactive traps to pattern multiple particle populations, showing interlaced (I; fluorescence and brightfield) bead populations, row-organized (II) bead populations, and arrays of beads and cells (III; green = cells; buffer solution = seruma-containing media, $\sigma \sim 1.5$ S/ma). (Scale bars = 100 μm).

retention [Fig. 2(c)]. For cases where beads were sized below this range, we routinely witnessed weir unloading where beads progressed laterally around the trap and swept out of the system with passing flow. Conversely, in cases where beads were sized larger than the optimal ~ 25 μm diameter range, we regularly saw expulsion via a vertical cascading mechanism where individual beads rotated over the weir tops and passed downstream (supplemental Fig. 3, size_selectivity.mpg).¹⁴

We observed that reduced flow rates enhanced loading for beads sized larger than our optimal capture range but did not affect loading for particles sized below this window [Fig. 2(c)]. We posit that the release mechanics for larger beads are explained by an imbalance between bead center heights and partnered weir heights. Here the bead centers are elevated above the top surfaces of the weirs, such that a drag-induced torque causes particle expulsion up and over the trap. Higher flow rates apply higher drag forces which in turn create more sizeable torques to enable particle extractions and reduce loading percentages. Conversely, we believe that particles sized below a critical threshold fail to disrupt local flows to an extent that could enable stable retention. We suspect that smaller particles are thereby more heavily influenced by streamlines that enter the capture crevices and then laterally wrap around the periphery of individual weirs.

To study the lower limits for particle capture, we ran assays with reduced flow rates and surveyed responses with SU-8-based weirs that offered better replication of the original mask features [Fig. 2(d)]. Though both the SU-8 and PPS designs demonstrated statistically significant increases in their site loading percentages when transitioning from 10 to 15 μm beads [1 and 3 in Fig. 2(d)], the retention percent-

ages for SU-8 weirs tested with 15 μm beads were even higher than the comparable PPS case [2 in Fig. 2(d)]. The difference in loading between the SU-8 and PPS-based structures suggests that slight alterations in geometry, whether they stem from the sidewall angle and/or the patterned radius of curvature of a chosen polymer can significantly modulate the ability to stably retain particles within the trap. In summary, our results suggest that large-gap weirs operate according to mechanics distinct from narrow-gap weirs and that their capture capabilities are sensitive to trap geometries that we can readily tune (supplemental Fig. 4).¹⁴

When used in combination with the on-chip activating electrodes, our platform provides two methods for microparticle organization. In an ejection response mode, we initially load all sites by deactivating the electrodes and flushing particle-laced fluid through the system. We then turn active array sites on by applying voltages to their affiliated electrodes. This procedure exerts vertical n -DEP forces on particles held in the weir capture crevices causing them to levitate above the weirs where they progress out of the device [Fig. 3(a)]. Such operations typically demand only a few seconds to, at most, 10 s of electrode activation to realize 100% particle ejection in typical experiments. Alternatively, using an exclusion response mode [Fig. 3(b)], we can prevent loading at active sites altogether by injecting particles into the device flow chamber with the electrodes in an on state that repels particles from the capture crevices. Both approaches use n -DEP to *repel* particles from loading sites, retaining particles that experience no DEP forces (basic_operations.mpg).¹⁴

In Fig. 3(c), we show a series of patterning results enabled by our approach. In I and II, we present a checkerboard formation of two interlaced fluorescent bead populations and the organization of three distinct bead types in separate rows. III further provides overlapping arrays of patterned K-562 cells and fluorescent beads. These results exemplify key functionalities that our *active* weir designs add to prior static weir-based efforts for enabling the organization of multiple particle types on a common substrate. As an added flexibility, the semicircular electrodes surrounding individual weirs can serve to “reset” held particles to the center of weir capture crevices (supplemental Fig. 5).¹⁴ When switching between injected populations of distinct particle types, this functionality proves especially useful for avoiding the possibility of dislodging populations loaded in prior stages of an assay.

Our work introduces an approach for manipulating micron-scale particles that capitalizes upon the efficient capture mechanics of large-gap weirs and augments that functionality using active n -DEP forcing. In a single platform we offer a means for ejecting and/or excluding particles from targeted subsets of arrayed system traps. We thus provide a scalable technology for sorting and positioning micron-scale particles that functions effectively in a wide variety of buffer types.

This work was supported in part by the NIH (Contract No. RR19652) and the Singapore-MIT Alliance. B.M.T. was partially supported by a NSF Graduate Research Fellowship and by the NIH Cell Decision Processes Center. We additionally thank the Microsystems Technology Laboratories at MIT and the W.M. Keck Foundation at the Whitehead Institute for valuable discourse and facilities access. Supplemental Information is available via the Electronic Physics Auxiliary Publication Service (EPAPS) of the American Institute of Physics.

¹Y. Yin, Y. Lu, and Y. Xia, *J. Mater. Chem.* **11**, 987 (2001).

²V. X. Nguyen and K. J. Stebe, *Phys. Rev. Lett.* **88**, 164501 (2002).

³T. A. Dickinson, K. L. Michael, J. S. Kauer, and D. R. Walt, *Anal. Chem.* **71**, 2192 (1999).

⁴D. R. Albrecht, V. L. Tsang, R. L. Sah, and S. N. Bhatia, *Lab Chip* **5**, 111 (2005).

⁵S. Fiedler, S. G. Shirley, T. Schnelle, and G. Fuhr, *Anal. Chem.* **70**, 1909 (1998).

⁶T. B. Jones, *Electromech of Particles*, 1st ed. (Cambridge University Press, New York, 1995).

⁷K. Ahn, C. Kerbage, T. P. Hunt, R. M. Westervelt, D. R. Link, and D. A. Weitz, *Appl. Phys. Lett.* **88**, 024104 (2006).

⁸D. S. Gray, J. L. Tan, J. Voldman, and C. S. Chen, *Biosens. Bioelectron.* **19**, 1765 (2004).

⁹D. Di Carlo, L. Y. Wu, and L. P. Lee, *Lab Chip* **6**, 1445 (2006).

¹⁰A. R. Wheeler, W. R. Thronset, R. J. Whelan, A. M. Leach, R. N. Zare, Y. H. Liao, K. Farrell, I. D. Manger, and A. Daridon, *Anal. Chem.* **75**, 3581 (2003).

¹¹C. M. Das, F. Becker, S. Vernon, J. Noshari, C. Joyce, and P. R. C. Gascoyne, *Anal. Chem.* **77**, 2708 (2005).

¹²B. M. Taff and J. Voldman, *Anal. Chem.* **77**, 7976 (2005).

¹³S. P. Desai, B. M. Taff, and J. Voldman, *Langmuir* **24**, 575 (2008).

¹⁴See EPAPS Document No. E-APPLAB-94-009908 for added information regarding specifics on our hydrodynamic weir-based device designs and operations as well as details relevant to the passive loading responses of such geometries. For more information on EPAPS, see <http://www.aip.org/pubservs/epaps.html>.